Structure and magnetism on iron oxide clusters Fe_nO_m (n = 1−5): Calculation from first principles

H. Shiroishi[1], T. Oda[1,a], I. Hamada[2], and N. Fujima[3]

[1] Department of Computational Science, Faculty of Science, Kanazawa University, Kanazawa 920-1192, Japan
[2] Division of Materials Physics, Department of Physical Science, Graduate School of Engineering Science, Osaka University, 1-3 Machikaneyama-cho, Toyonaka 560-8531, Japan
[3] Faculty of Engineering, Shizuoka University, Hamamatsu 432-8561, Japan

Abstract. We have studied structural and magnetic properties in small iron oxide clusters, Fe_nO_m ($n = 1-5$), by means of the first–principles calculation based on the density functional theory. We have used not only the usual spin polarized scheme, but also the scheme for noncollinear magnetism to carry out efficient optimization in magnetic structure. The result of FeO_m ($m = 1-4$) is in good agreement with the previous work. We found the stable adduct clusters in FeO_5 and FeO_6. The bridge site of oxygen atom is more favorable in energy than any other site for the clusters of Fe_nO ($n = 2-5$). As increasing the number of oxygen atoms, the alignment of Fe magnetic moments changes from ferromagnetic configuration to antiferromagnetic one at Fe_nO_n ($n = 2-4$).

PACS. 61.46.+w Nanoscale materials: clusters, nanoparticles, nanotubes, and nanocrystals –
75.75.+a Magnetic properties of nanostructures – 71.15.Pd Molecular dynamics calculations
(Car-Parrinello) and other numerical simulations

1 Introduction

Magnetic clusters are the candidate of magnetic nano size material for the high density magnetic memory storage or the spintronics of semiconductors. To practically use the clusters as a nano magnetic material, it is important to study the effect of oxidation on the structure and magnetism of the clusters.

The number of experimental studies for iron oxide clusters have increased since the middle of 1990s. Wang and co-workers have been performed the systematic studies for electronic structures by using a photoelectron spectroscopy [1–3]. Their important result is the electron affinity of anion clusters. They have tried to approach structural properties, combined with an electrostatic model [1] and an *ab initio* local-spin-density calculation [2]. Griffin *et al.* studied the reaction of iron cation clusters with oxygen with using a guided ion beam mass spectrometer [4]. They found that the dioxide cation clusters dominate the product. The groups of Sumiyama and Kawazoe have devoted their collaboration to the study on magic numbers in iron oxide clusters [5–7]. Gutsev *et al.* studied the electronic and geometrical structures of multi-oxide mono-iron clusters with using a density functional theory. They

also calculated vibrations, electron affinities, and thermodynamic stabilities [8]. In these works above, however, there is no theoretical study on multi-oxide multi-iron-atom clusters, even for ground state structural properties.

Iron oxide compound in bulk is known to have variety of structural and magnetic properties; FeO has a rocksalt structure and shows an antiferromagnetic order at low temperatures, Fe_3O_4 (magnetite) a spinel-structure and a ferrimagnetic order, and Fe_2O_3 (hematite) a corundum structure and an essentially antiferromagnetic order. In these compounds iron atoms are separated by O atoms ($d_{Fe-Fe} \sim 3$ Å) and there is no direct bond between iron atoms. This separation causes the tendency of antiferromagnet in the oxide bulk rather than that of ferromagnet. The latter is found in the pure iron bulk and the pure iron clusters [9,10]. Because ferromangnetic clusters are available for magnetic devices, it is important to know transitions from ferromagnet to antiferromagnet in oxide clusters.

We have studied structural and magnetic properties in iron oxide clusters, Fe_nO_m ($n = 1-5$), with using a first–principles molecular dynamics [11]. In the next section the calculation method is briefly addressed, in Section 3 we present results and discussions and in Section 4 we summarize the work.

[a] e-mail: oda@cphys.s.kanazawa-u.ac.jp

2 Calculation method

We have used the first principles molecular dynamics [11], which is based on the density functional theory [12]. We employed the ultra-soft pseudo potentials [13,14] and planewaves. Our scheme used allows us to take the simultaneous optimization in both of atomic and electronic freedoms. The clusters are placed in a cubic cell of side 20 a.u. The energy cutoffs are 24 Ry for the planewave expansion of wavefunctions at the Γ point and 250 Ry for the augmented electron density [14]. We used the generalized gradient approximation for the exchange-correlation energy [15]. To treat the metallic property that there are some degenerate states around the Fermi level, we introduced the additional freedom of partial occupations [16–18], which gives reasonable trajectories on electronic level crossings at the Fermi level [19]. We used a value of 0.2 eV for the level smearing at the Fermi level. Consequently, this treatment resulted in non-integer values for the magnetizations which are obtained by integrating spin densities.

In pure iron clusters, there are ferromagnetic and antiferroamgnetic interactions between magnetic moments on atoms and they are sensitive to the distance between atoms [20,21]. Due to this fact, noncollinear magnetic structures could appear at stable clusters or in the optimization process of atomic and electronic configurations. Therefore, we have also used the scheme of noncollinear magnetism [20] as well as the usual spin polarized scheme for density functional calculations.

3 Results and discussion

In this work, we considered only the oxide clusters in which O atoms could be arranged on iron clusters.

3.1 FeO$_m$ (m = 1−6)

The optimized FeO cluster has the bond length of 1.63 Å and the magnetization of $4.1\mu_B$. The three clusters are obtained for FeO$_2$; the most stable is the obtuse isosceles triangle (apex angle 121°) with $3.3\mu_B$, the next stable cluster has the OFeO linear structure with smaller magnetization ($1.7\mu_B$). The acute geometry (apex angle 47°) is less binding with larger magnetization ($4.5\mu_B$).

For $m = 3$ and 4, the respective ground state clusters are of nonmagnetic state, which agrees with the results of Gutsev *et al.* [8]. The most stable cluster has a plane structure with D_{3h} symmetry for $m = 3$ and a tetrahedral cage of O atoms with a centered Fe atom for $m = 4$.

In the stable clusters of $m = 5$ and 6, the number of direct bonds between Fe and O atoms is 4. The clusters obtained could be regarded as an adduct with O$_2$. Especially, for $m = 5$, the binding energy between O$_2$ and FeO$_3$ is found to be ~0.4 eV, much smaller than the bonding energies between Fe and O atoms (3−5 eV). It is interesting that the magnetization of O$_2$ couples anti-parallel with that induced on Fe atom in the FeO$_3$ although the corresponding isolated FeO$_3$ cluster is nonmagnetic.

(a) Fe$_2$O
8.1 eV, $6.8\mu_B$

(b) Fe$_2$O$_2$
14.0 eV, $0.0\mu_B$

(c) Fe$_2$O$_2$
13.9 eV, $6.4\mu_B$
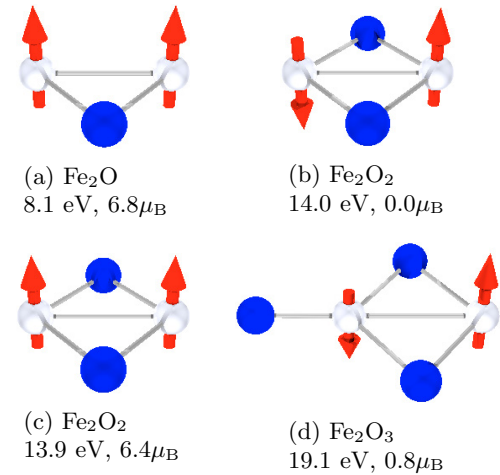
(d) Fe$_2$O$_3$
19.1 eV, $0.8\mu_B$

Fig. 1. The geometries and magnetic arrangements of FeO$_m$ ($m = 1-3$). The gray and filled balls specify Fe and O atoms, respectively. The arrows show atomic magnetic moments. The binding energy and the total magnetization are also presented.

3.2 Fe$_2$O$_m$ (m = 1−6)

We show the geometries and magnetic arrangements of typical clusters in Figure 1. The arrows represent atomic magnetic moments, which were estimated by integrating spin densities within radii of 0.90 and 0.69 Å on Fe and O atoms, respectively. The magnetization on O atoms does not appear in the figure due to their small values.

For Fe$_2$O, an O atom is added to the bridge site between two Fe atoms or the edge site which forms a linear cluster. The cluster with the bridge O atom is the most stable and has a ferromagnetic arrangement in Fe magnetic moments, similar to the pure Fe$_2$ cluster. The O atom at edge site induces the antiferromagnetic arrangement, resulting in the cluster which is higher in energy by 1.1 eV.

The additional O atom at an bridge site for Fe$_2$O$_2$ make two stable magnetic arrangements; ferromagnetic (Fig. 1c) and antiferromagnetic (Fig. 1b) clusters with the similar planar geometry. The latter is more stable by 0.15 eV than the former and has a longer Fe-Fe bond by 0.08 Å. For Fe$_2$O$_3$ the cluster with two O atoms at the bridge and an O atom at the edge (Fig. 1d) was obtained as the most stable one. Such a double-bridge structure is preserved in low-energy clusters for Fe$_2$O$_m$ ($m \geq 4$). The most stable cluster of Fe$_2$O$_6$ is nonmagnetic, in agreement with the argument that the cluster has twice stoichiometry of FeO$_3$.

In Figure 2, we show the oxidation dependence of total magnetization for Fe$_2$O$_m$. The change from the ferromagnet to antiferromagnet appears at Fe$_2$O$_2$ in the sequence of the ground state geometry.

3.3 Fe$_3$O$_m$ (m = 1−5)

The ground state geometry of Fe$_3$ is a regular triangle. The stable sites for O atoms are the bridge sites, and the
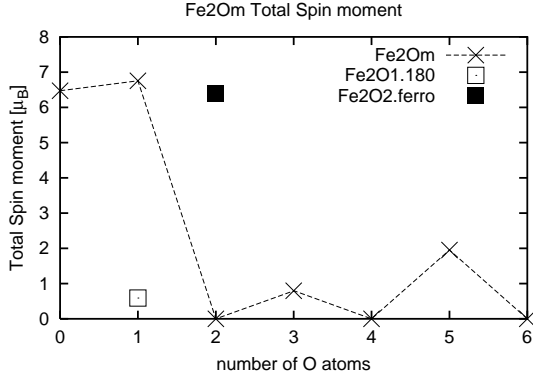
Fig. 2. The oxidation dependence of total magnetization for Fe_2O_m. The crosses specify data of the most stable cluster, connected with the broken lines. The empty square specifies data of the linear cluster in Fe_2O and the filled square data of ferromagnetic arrangement in Fe_2O_2.

(a) Fe_3O ($n_b = 1$) 11.3 eV, $10.2\mu_B$ (b) Fe_3O ($n_s = 1$) 10.8 eV, $10.1\mu_B$ (c) Fe_3O_2 ($n_b = 2$) 17.5 eV, $11.6\mu_B$

(d) Fe_3O_2 ($n_b = 1$, $n_s = 1$), 16.7 eV, $10.5\mu_B$ (e) Fe_3O_2 ($n_s = 2$) 16.4 eV, $11.3\mu_B$ (f) Fe_3O_3 ($n_b = 3$) 24.0 eV, $3.4\mu_B$

(g) Fe_3O_4 ($n_b = 3$, $n_s = 1$), 28.3 eV, $4.0\mu_B$ (h) Fe_3O_5 ($n_b = 3$, $n_s = 2$), 31.5 eV, $0\mu_B$

Fig. 3. The geometries and magnetic structures of Fe_3O_m ($m = 1{-}5$).

surface sites, that is, the sites on the center of the triangle. When adding an O atom, we obtained two stable structures; Fe_3O ($n_b = 1$) in Figure 3a, where n_b is the number of O atoms at bridge sites, and Fe_3O ($n_s = 1$) in Figure 3b, where n_s is the number of O atoms at surface sites. The former ($n_b = 1$) is more stable by 0.5 eV than the latter ($n_s = 1$). The addition of an O atom extends the bond length between the bridged Fe atoms by 10% for $n_b = 1$, and the edge lengths of the triangle by 5% for $n_s = 1$.

In Fe_3O_2, the most stable cluster is obtained for $n_b = 2$ in Figure 3c, which has the larger magnetization ($11.6\mu_B$). The second stable one is for $n_b = n_s = 1$ in Figure 3d, and the third one is for $n_s = 2$ in Figure 3e. Both of these clusters also have a larger magnetization ($11{-}12\mu_B$).

In $Fe_3O_m (m \geq 3)$, the configuration of $n_b = 2$ and $n_s = 1$ is unstable, and three O atoms at the bridge sites ($n_b = 3$) form the stable clusters. This result greatly supports the occupation sequence, proposed by Wang *et al.* [1], that the O atoms occupy all the three bridge sites at first. As increase of O atoms, ferromagnetic arrangement in clusters changes to ferrimagnetic one. As shown in Figure 4, it results in a smaller total magnetization equal or less than $4\mu_B$ for Fe_3O_3 and Fe_3O_4, and $0\mu_B$ for Fe_3O_5 ($n_b = 3, n_s = 2$). It is interesting to find the cluster with the noncollinear magnetic structure for Fe_3O_5 (Fig. 3h).

3.4 Fe_4O_m ($m = 1{-}6$) and Fe_5O_m ($m = 1, 2$)

The ground state geometry of Fe_4 is a tetrahedron. In the clusters of Fe_4O, the bridge site is more stable for O atom than the surface site (see Figs. 5a and 5b). However, in Fe_4O_2, the cluster for $n_b = n_s = 1$ in Figure 5c is lower in energy by 0.2 eV than that for $n_b = 2$ in Figure 5d. The cluster with double surface atoms in Fe_4O_2 has a higher energy than the two previous clusters. It was also found that the Fe_4O_3 ($n_b = 3$) is less stable than Fe_4O_3 ($n_b = 2, n_s = 1$). The stable structure in Fe_4O_4 shows
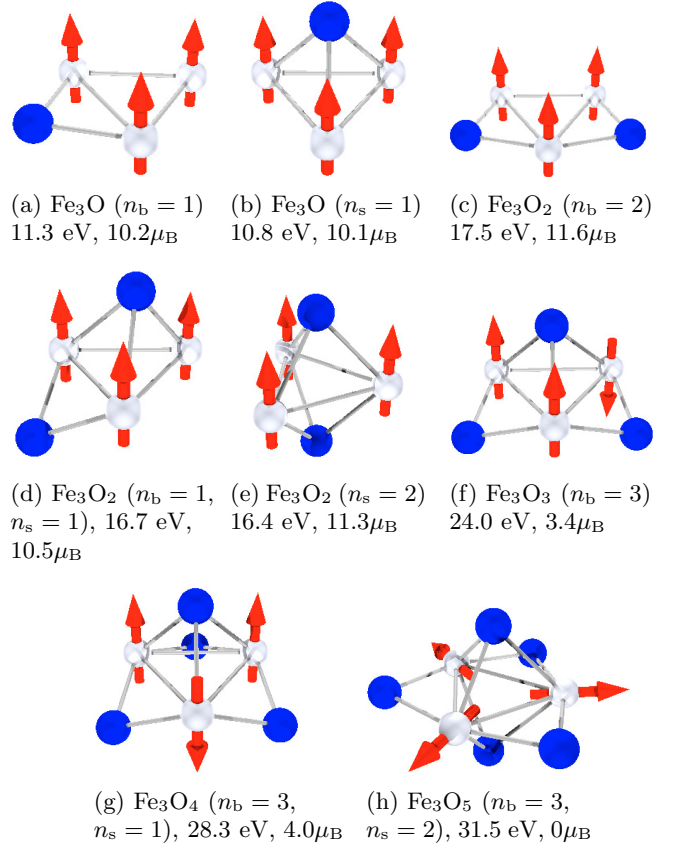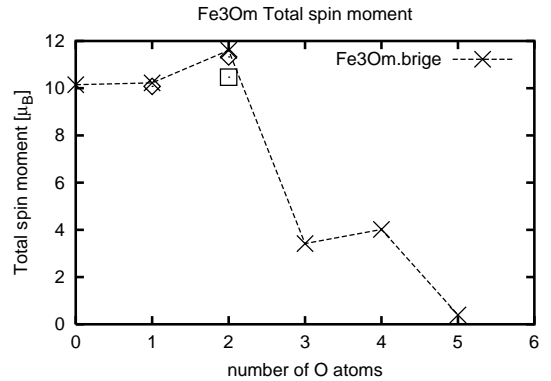

Fig. 4. The oxidation dependence of total magnetization for Fe_3O_m. The crosses specify data of the most stable cluster, connected with the broken lines. The diamonds specify data of clusters only with surface O atoms and the square the cluster with one bridge and one surface O atoms.

a relatively larger distortion of the tetrahedron and an antiferromagnetic arrangement in Fe moments (Fig. 6).

For Fe_5O_m, the oxidation effects are similar to those of Fe_4O_m. The bridge site is lower in energy than the surface site in oxidation of the first atom, and for Fe_5O_2, the cluster of double bridges is not the most stable. The magnetic arrangements are still ferromagnetic within $m = 1$ and 2.
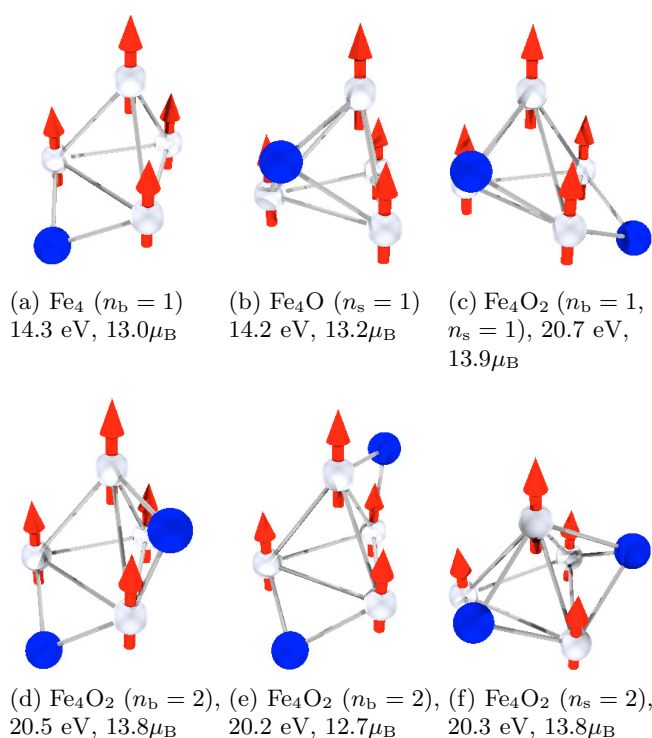
(a) Fe_4 ($n_b = 1$) 14.3 eV, 13.0μ_B

(b) Fe_4O ($n_s = 1$) 14.2 eV, 13.2μ_B

(c) Fe_4O_2 ($n_b = 1$, $n_s = 1$), 20.7 eV, 13.9μ_B

(d) Fe_4O_2 ($n_b = 2$), 20.5 eV, 13.8μ_B

(e) Fe_4O_2 ($n_b = 2$), 20.2 eV, 12.7μ_B

(f) Fe_4O_2 ($n_s = 2$), 20.3 eV, 13.8μ_B

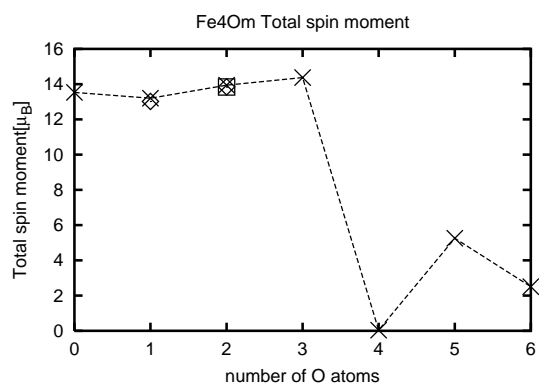**Fig. 5.** The geometries and magnetic structures of Fe_4O_m ($m = 1-2$).

Fig. 6. The oxidation dependence of total magnetization for Fe_4O_m. The crosses specify data of the most stable cluster, connected with the broken lines. The diamonds specify data of the clusters only with surface O atoms and the square with one bridge and one surface O atoms.

4 Summary

We have carried out the geometrical and magnetic optimization for the iron oxide clusters, Fe_nO_m ($n = 1-5$), with using the first–principles molecular dynamics. We have used not only the usual spin polarized scheme, but also the scheme for noncollinear magnetism. We found the noncollinear magnetic structure in Fe_3O_5. The results of FeO_m ($m = 1-4$) are in good agreement with the previous work. We also found the stable adduct clusters in FeO_5 and FeO_6. For Fe_2O_m ($m = 2$), ferro- and antiferromagnetic clusters are found as stable cluster, having similar structural geometries. For Fe_nO ($n = 2-5$), the bridge site is lower in energy than the surface site for the first oxidation with O atom. On such a single-O bridged clusters, the second O atom favors a bridge site in Fe_3O_2 and a surface site in Fe_nO_2 ($n = 4, 5$). Increasing the number of oxygen atoms, the alignment of Fe magnetic moments changes from ferromagnetic arrangement to antiferromagnetic one at $m = n$ for $n = 2, 3$, and 4.

References

1. L.S. Wang, H. Wu, S. Desai, Phys. Rev. Lett. **76**, 4853 (1996)
2. L.S. Wang, J. Fan, L. Lou, Surf. Rev. Lett. **3**, 695 (1996)
3. J. Fan, L.S. Wang, J. Chem. Phys. **102**, 8714 (1995)
4. J.B. Griffin, P.B. Armentrout, J. Chem. Phys. **106**, 4448 (1997)
5. Q. Sun, Q. Wang, K. Parlinski, J.Z. Yu, Y. Hashi, X.G. Gong, Y. Kawazoe, Phys. Rev. B **61**, 5781 (2000)
6. Q. Sun, M. Sakurai, Q. Wang, J.Z. Yu, G.H. Wang, K. Sumiyama, Y. Kawazoe, Phys. Rev. B **62**, 8500 (2000)
7. Q. Wang, Q. Sun, M. Sakurai, J.Z. Yu, B.L. Gu, K. Sumiyama, Y. Kawazoe, Phys. Rev. B **61**, 5781 (1999)
8. G.L. Gutsev, S.N. Khanna, B.K. Rao, P. Jena, J. Phys. Chem. A **103**, 5812 (1999)
9. I.M.L. Billas, A. Chatelain, W.A. de Heer, Science **265**, 1682 (1994)
10. O. Diéguez, M.M.G. Alemany, C. Rey, P. Ordejón, L.F. Gallego, Phys. Rev. B **63**, 205407 (2001)
11. R. Car, M. Parrinello, Phys. Rev. Lett. **55**, 2471 (1985)
12. P. Hohenberg, W. Kohn, Phys. Rev. B **136**, 864 (1964); W. Kohn, L.J. Sham, Phys. Rev. A **140**, 1133 (1965)
13. D. Vanderbilt, Phys. Rev. B **41**, 7892 (1990)
14. A. Pasquarello *et al.*, Phys. Rev. Lett. **69**, 1982 (1992); K. Laasonen *et al.*, Phys. Rev. B **47**, 10142 (1993)
15. J.P. Perdew *et al.* Phys. Rev. B. **46**, 6671 (1992)
16. N.D. Mermin, Phys. Rev. B **137**, A1441 (1965)
17. N. Marzari, D. Vanderbilt, M.C. Payne, Phys. Rev. Lett. **79**, 1337 (1997)
18. T. Oda, J. Phys. Soc. Jpn **71**, 519 (2002)
19. S. Kawamoto, T. Oda, I. Hamada, Int. J. Quant. Chem. **91**, 165 (2003)
20. T. Oda, A. Pasquarello, R. Car, Phys. Rev. Lett. **80**, 3622 (1998)
21. N. Fujima, T. Oda, Trans. Mat. Res. Soc. Jpn **27**, 201 (2002)